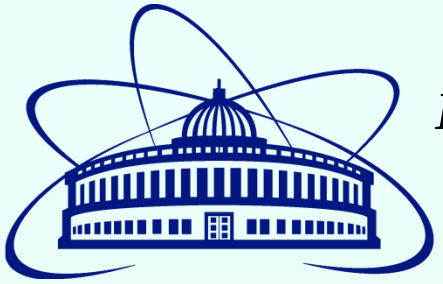

Bogoliubov Laboratory of Theoretical Physics
Joint Institute for Nuclear Research

Van der Waals He and Ne three-body systems and Efimov states

E.A. Kolganova, R.V.Jolos
BLTP JINR

Nucleus-2025
June 30 – July 6, 2025, St.Petersburg

Outline

- What is known about Helium and Neon
- Dimers – Experiments, Potentials, Theory
- Trimers – Experiments, Theory
- Summary

Helium

- The inertness of the helium atom is responsible for the **an extremely weak van der Waals interaction** between two helium atoms, which was a reason for a long standing debates about existence of the helium dimer, until it was experimentally observed in 1990s.

Molecules in Superfluid Helium Nanodroplets
Spectroscopy, Structure, and Dynamics
Ed.: A.Slenczka & J.P. Toennies (Springer,2022) **Topics in Applied Physics, V. 145**

Matter wave diffraction experiment

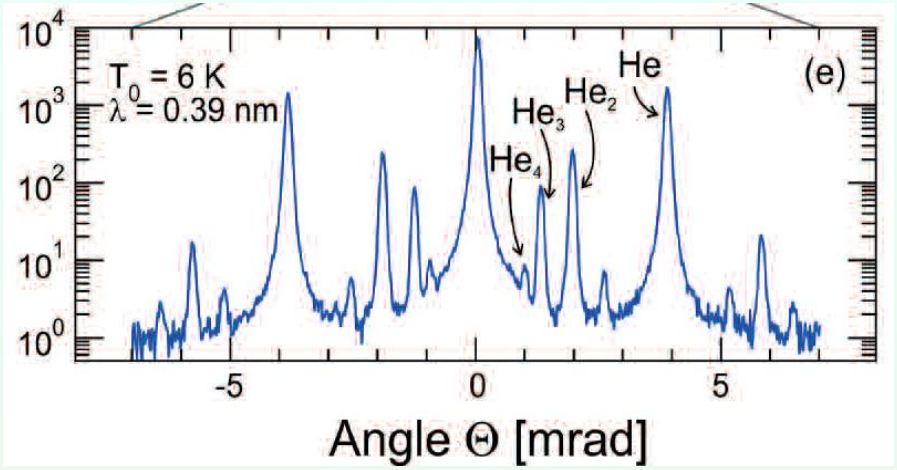

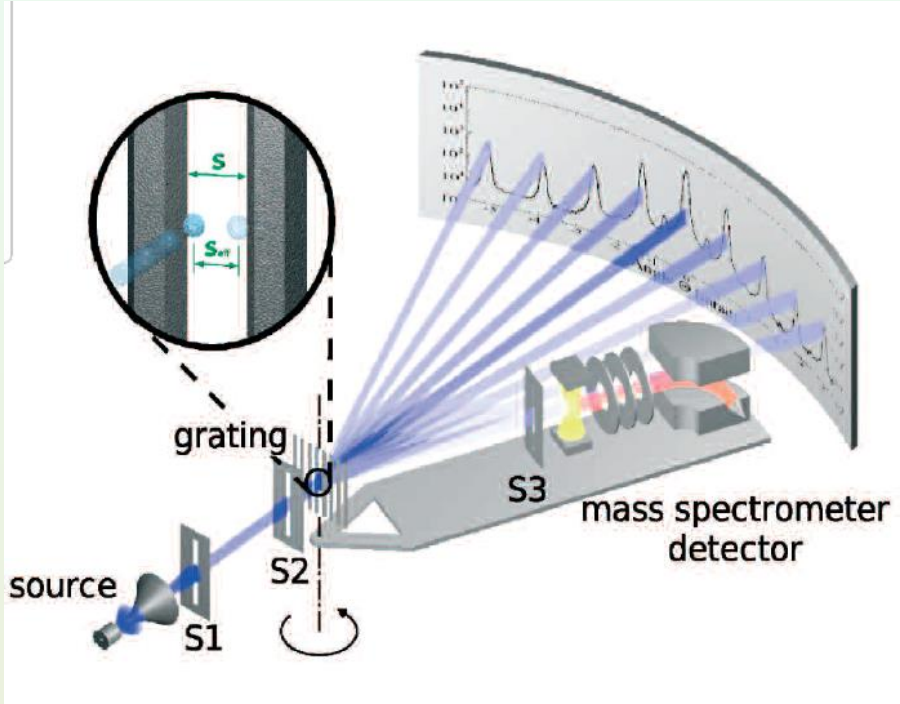

Louis de Broglie wavelength

$$\lambda = \frac{h}{M\,v}$$

The Diffraction angle

$$\sin\theta = n\,\frac{\lambda}{d} = n\,\frac{h}{d\,N\,m\,v}$$

m – mass of helium atom

N – number of helium atoms

$M = N\,m$ – mass of cluster

v – velocity

n – diffraction order

Schematic diagram of the cluster beam apparatus used for the diffraction of small He clusters in nozzle beam expansion exps.

Schoellkopf&Toennies, Science 266, 1345 (1994); Kornilov&Toennies doi: 10.1051/epn:2007003

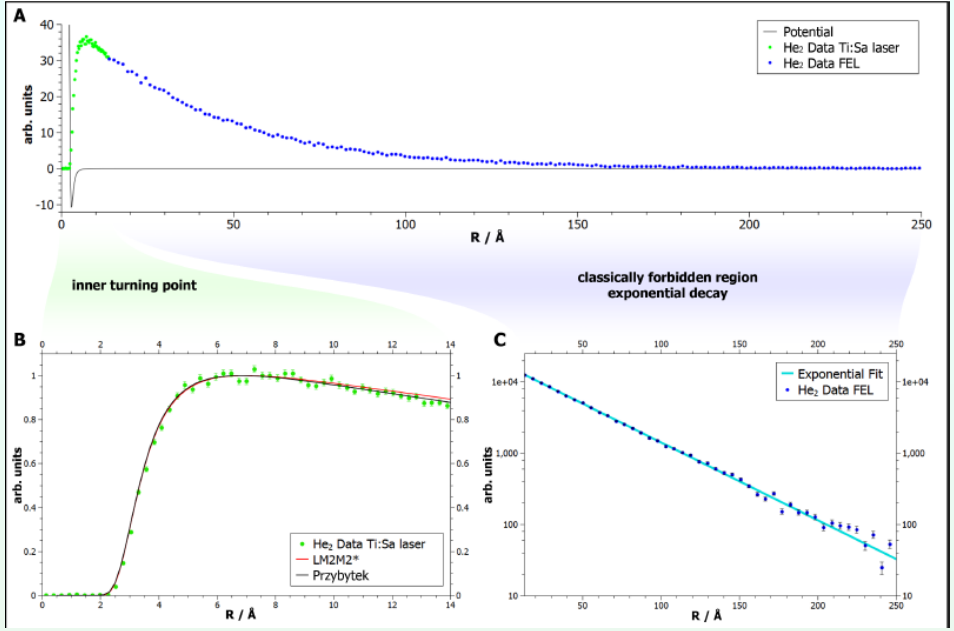

Experimental measurement of the helium dimer wavefunction (A).
Two detailed views show the important features of this quantum system: The region of the inner turning point (B) is in agreement with theoretical predictions with LM2M2 and Przybytek potentials, and the exponential decay in the classical forbidden region (C).
A helium dimer binding energy of **151.9 ± 13.3 neV ($1.76^{+0.15}_{-0.15}$ mK)** is obtained from the exponential slope.

$$\langle R \rangle = 52 \pm 4 \ \text{Å}$$

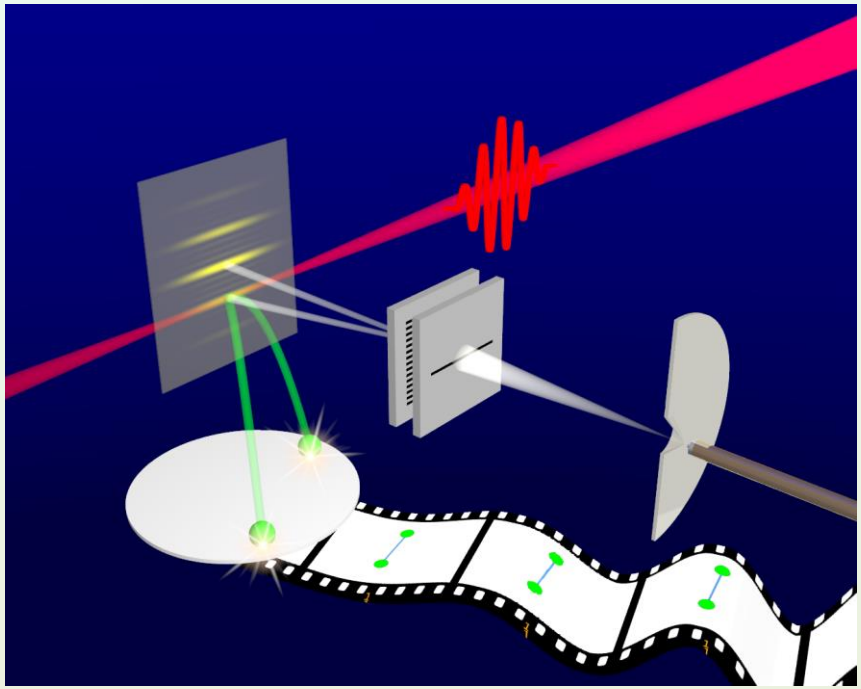

FLASH's X-rays (red) ionize both helium atoms of the molecule, causing them to separate in an explosive manner. The ions are then imaged on a location-resolving detector, symbolised by the film strip. The wave function is then reconstructed from a multitude of individual images.

S. Zeller, M. Kunitski, … R.Dörner, *PNAS*, 2016

INTERACTION POTENTIALS

$^4He_2$

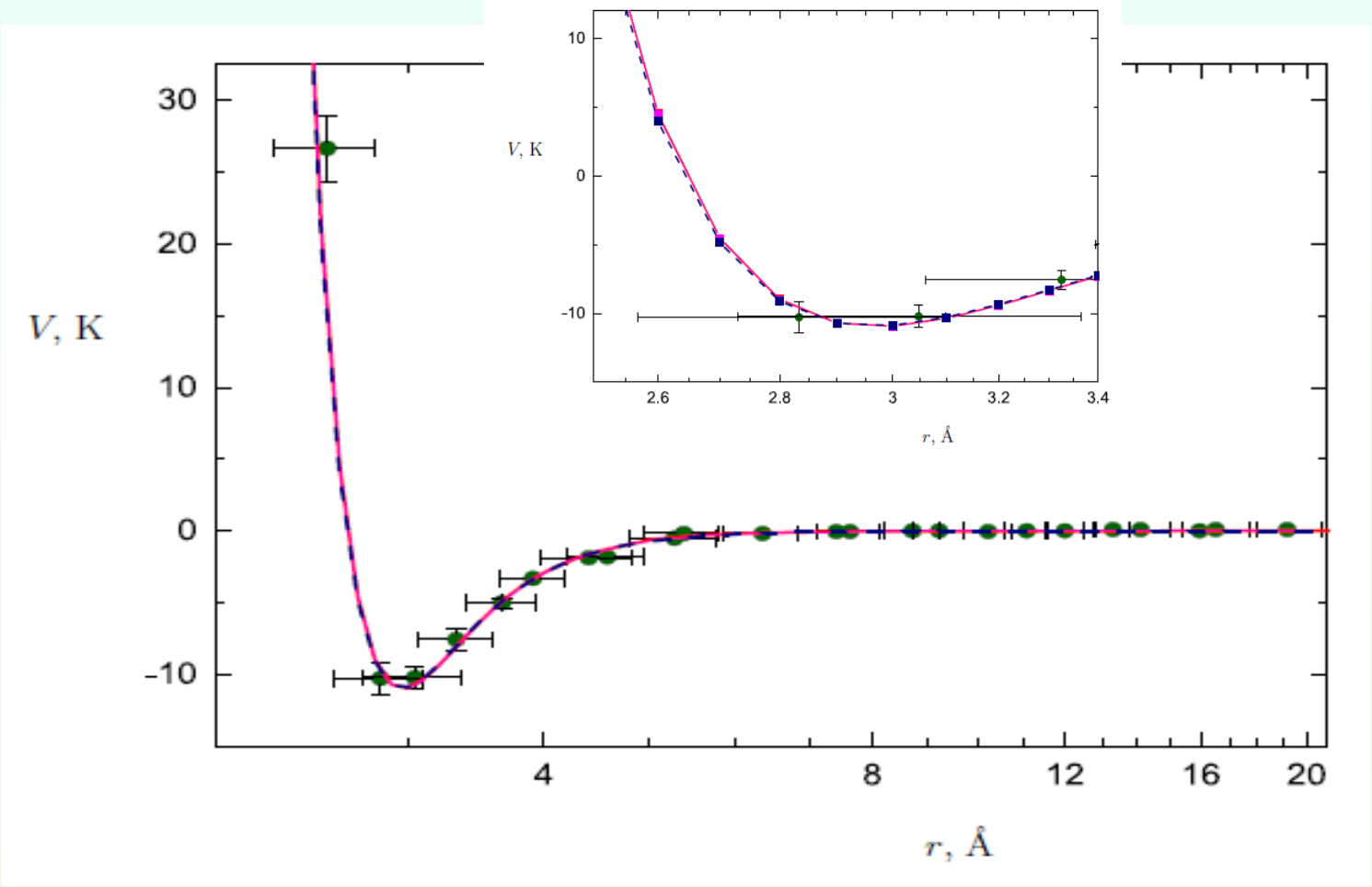

He-He potential V (r) , points are experimental data from **S. Zeller et al.** **Phys. Rev. Lett 121 (2018) 083002**, blue curve – HFD-B potential (by R.A.Aziz et al.), red curve – PRZ2010 (by M. Przybytek et al.).

INTERACTION POTENTIALS

Potential models:

– Lennard - Jones [1]: $V(r) = 4\,\varepsilon \left[\left(\frac{\sigma}{r}\right)^{12} - \left(\frac{\sigma}{r}\right)^{6}\right]$

ε – scales the energy and σ – the length scale;

– Tang -Toennies [2]: $V(R) = V_{rep} + V_{att} = A\,e^{-bR} - \sum_{n=3}^{N} f_{2n}(bR)\frac{C_{2n}}{R^{2n}}$

where A and b parameters,
the C_{2n} are the dispersion coefficient,
$f_{2n}(bR)$ - the damping function,
which is given by the following expression:

$$f_{2n}(x) = 1 - e^{-x}\sum_{k=0}^{2n}\frac{x^{-k}}{k!}$$

– Aziz [3]: $V(x) = \varepsilon\, V_b(\zeta)$

where $\zeta = x/r_m$, and term $V_b(\zeta)$ has the form:

$$V_b(\zeta) = A\exp(-\alpha\,\zeta + \beta\,\zeta^2) - \left[\frac{C_6}{\zeta^6} + \frac{C_8}{\zeta^8} + \frac{C_{10}}{\zeta^{10}}\right] F(\zeta)$$

at that $x$is expressed in the same length units as r_m(for this case they are angstroms).
Function $F(\zeta)$ is given by the expression:

$$F(\zeta) = \begin{cases} exp[-(D/\zeta - 1)^2], & if\ \zeta \le D, \\ 1, & if\ \zeta > D. \end{cases}$$

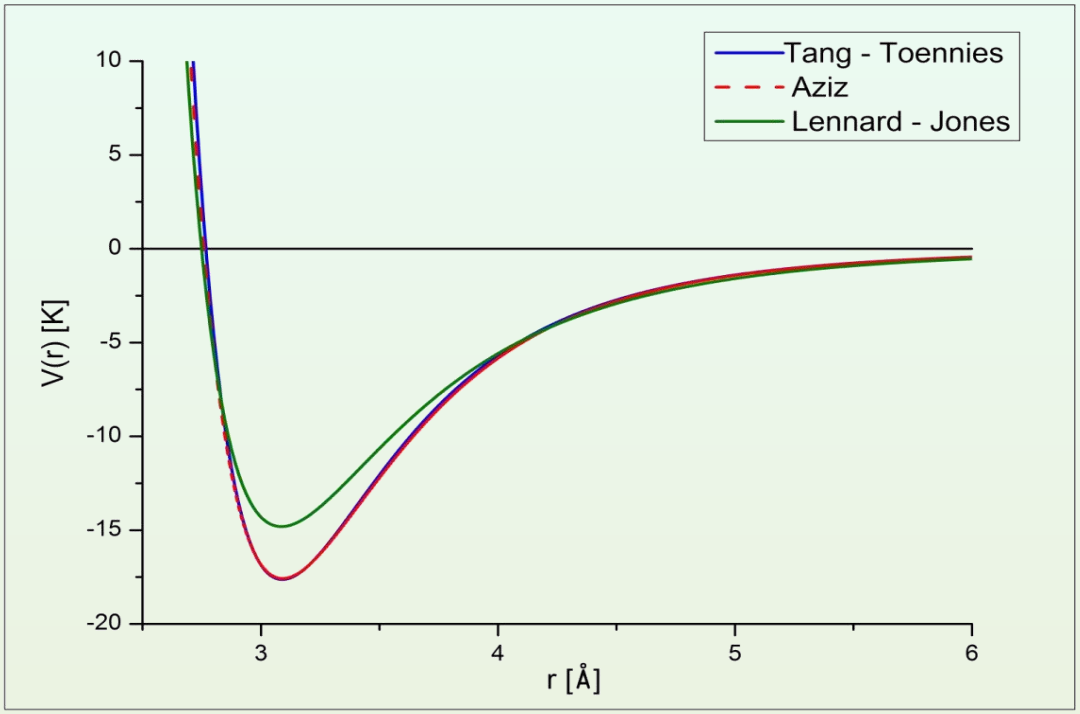

[1] J.E.Jones // Proc.R.Soc.London, ser A **106**, 463 (1924).
[2] K.T.Tang and J.P.Toennies // J.Chem.Phys.**118**, 4976 (2003).
[3] R.A.Aziz and M.J.Slaman // J.Chem.Phys.**94**, 8047 (1991); R.A.Aziz // J.Chem.Phys. **99**, 4518 (1993).

Potential models: PRZ2010 [6] and PRZ2017 [7]

$$V(R) = V_{BO}(R) + V_{ad}(R) + V_{rel}(R) + V_{QED}(R)$$

$V_{BO}(R)$ - nonrelativistic Born - Oppenheimer (BO),
$V_{ad}(R)$ - adiabatic correction,
$V_{rel}(R)$ - relativistic correction,
$V_{QED}(R)$ - quantum electrodynamics (QED).

R	V_{BO}	V_{ad}	V_{rel}	V_{QED}	V
3.0	3767.681(71)	1.387(7)	−0.2197(23)	0.0942(2)	3768.94(7)
4.0	292.570(15)	0.1080(32)	0.0324(14)	0.0089(2)	292.719(15)
5.0	−0.4754(65)	−0.0075(13)	0.0240(2)	−0.001 06(4)	−0.460(7)
5.6	−11.0006(2)	−0.0090(5)	0.015 40(4)	−0.001 35(2)	−10.9955(5)
6.0	−9.6819(23)	−0.0072(3)	0.011 43(5)	−0.001 20(4)	−9.6788(23)
7.0	−4.6225(6)	−0.003 33(7)	0.005 77(3)	−0.000 74(3)	−4.6208(6)
12.0	−0.165 92(2)	−0.000 125(1)	0.000 575(2)	−0.000 13(3)	−0.165 60(3)

The computed values of *V(R)* were fitted to an analytic function

$$\sum_{k=1}^{M} e^{-a_k R} \sum_{i=I_0}^{I_1} P_{ik} R^i - \sum_{n=N_0}^{N_1} f_n(\zeta R) \frac{C_n}{R^n}$$

$f_{2n}(x)$ - *the Tang-Toennies damping function*

$$f_{2n}(x) = 1 - e^{-x} \sum_{k=0}^{2n} \frac{x^{-k}}{k!}$$

a_k, P_{ik} and ζ are adjustable parameters, and the summation limits [M, I_0, I_1, N_0, N_1]

[6] Przybytek M., Cencek W., et. al. // Phys. Rev. Lett. 2010. 104. P. 183003.
[7] Przybytek M., Cencek W., et. al. // Phys. Rev. Lett. 2017. 119. P. 123401.

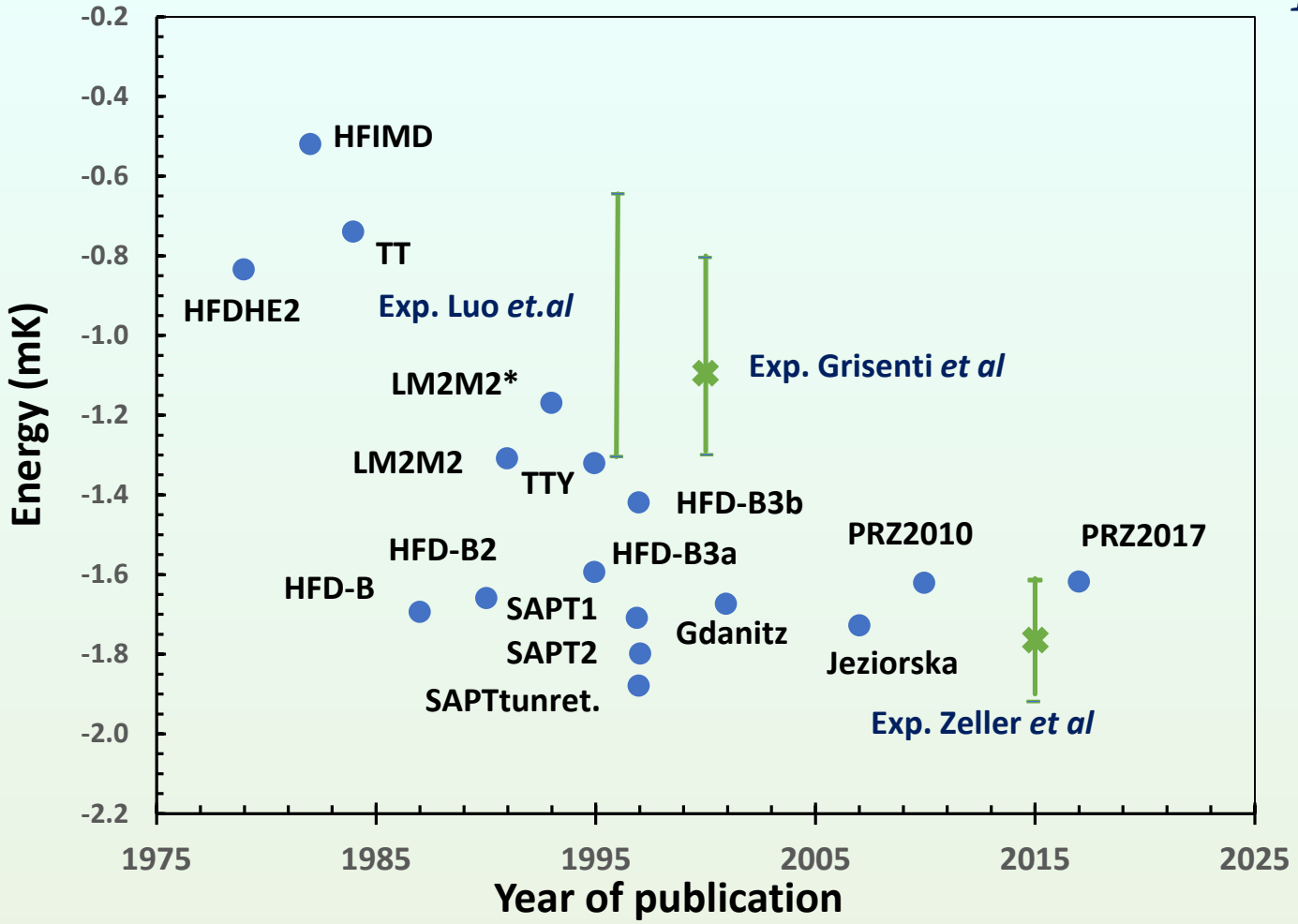

The predicted values for the helium dimer binding energy using theoretical calculations are displayed alongside experimental measurements

Idea by S. Zeller *et al.*//arXiv: 1601.03247

INTERACTION POTENTIALS

$^4He_2$

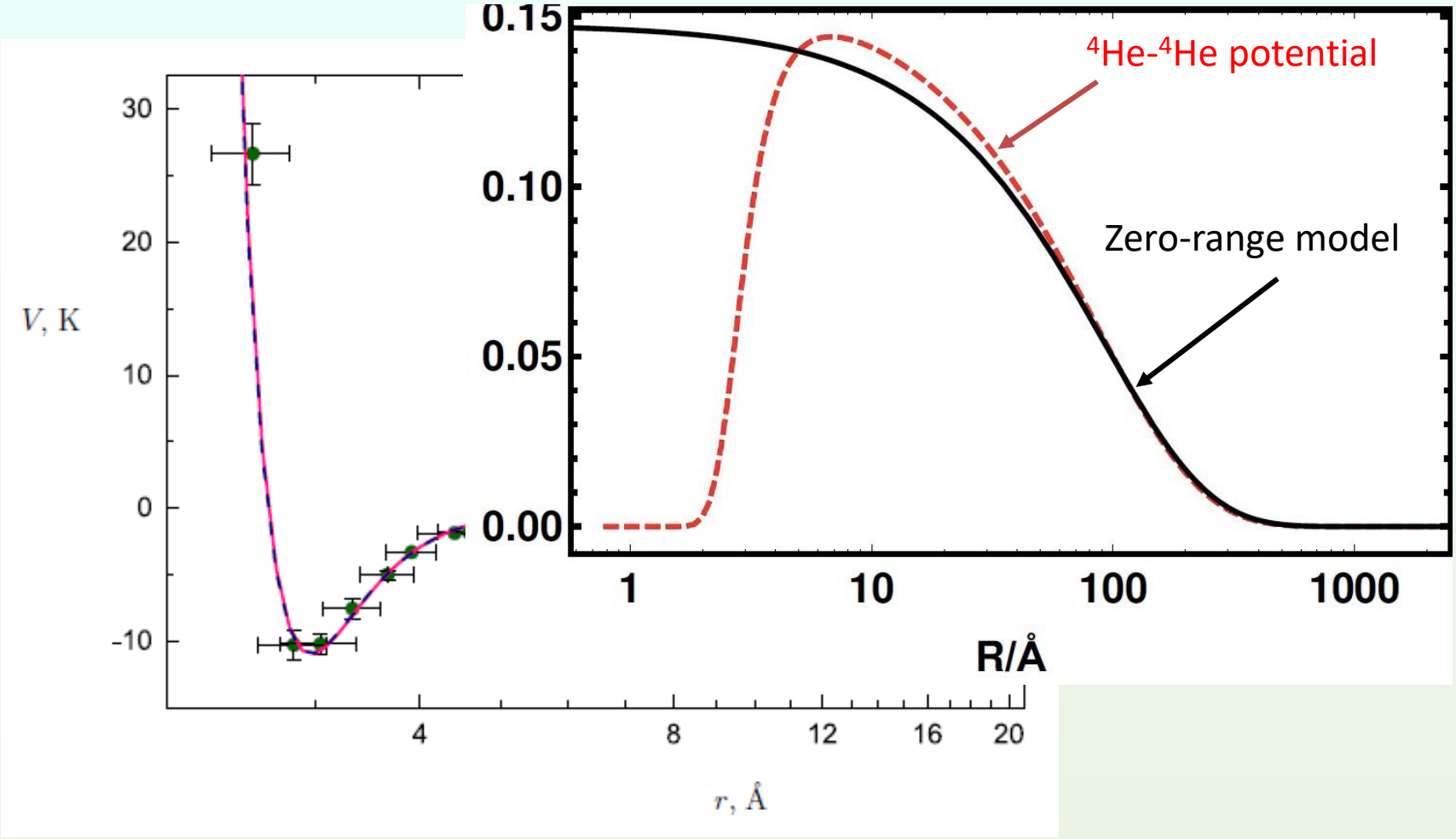

He-He potential V (r) , points are experimental data from **S. Zeller et al.** **Phys. Rev. Lett 121 (2018) 083002**, blue curve – HFD-B potential (by R.A.Aziz et al.), red curve – PRZ2010 (by M. Przybytek et al.).

Helium dimer

$^4He_2$

Bound state energy - $\varepsilon_d \approx -1.7\ mK$

No rotational J>0 bound states

^{3}He-^{4}He does not support bound states

Two-body s-wave scattering length $l_{sc} = 100^{+8}_{-7.9}$ Å

Two-body effective range $r_s \approx 7.2$ Å

1 K = 8.6 x 10^{-5} eV

HeNe dimer experiment

J. Kruse et al. // *J. Phys. Chem. Lett.* 2025, 16, 13, 3225-3231

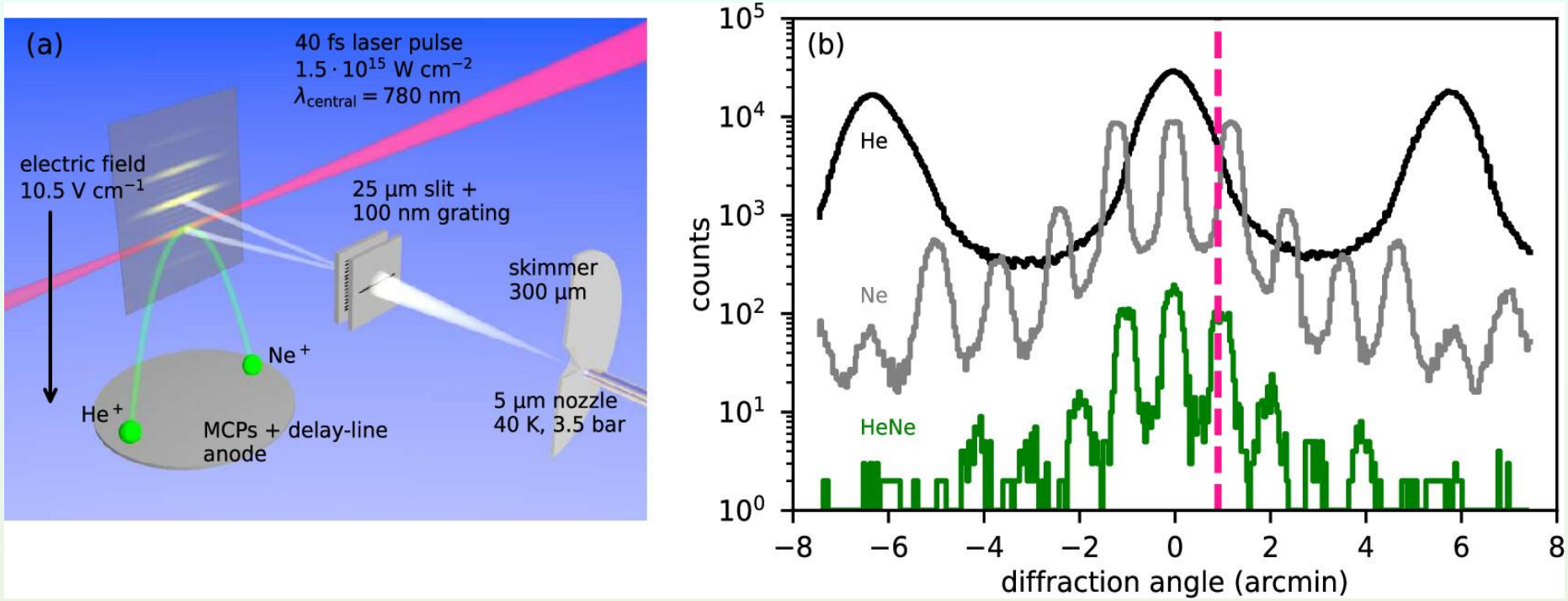

(a) Sketch of the experimental setup (see the text for details). (b) Measured diffraction patterns of single helium atoms (black curve), single neon atoms (gray curve), and helium–neon dimers (green curve).

INTERACTION POTENTIALS

$^{4}He\ ^{20}Ne$

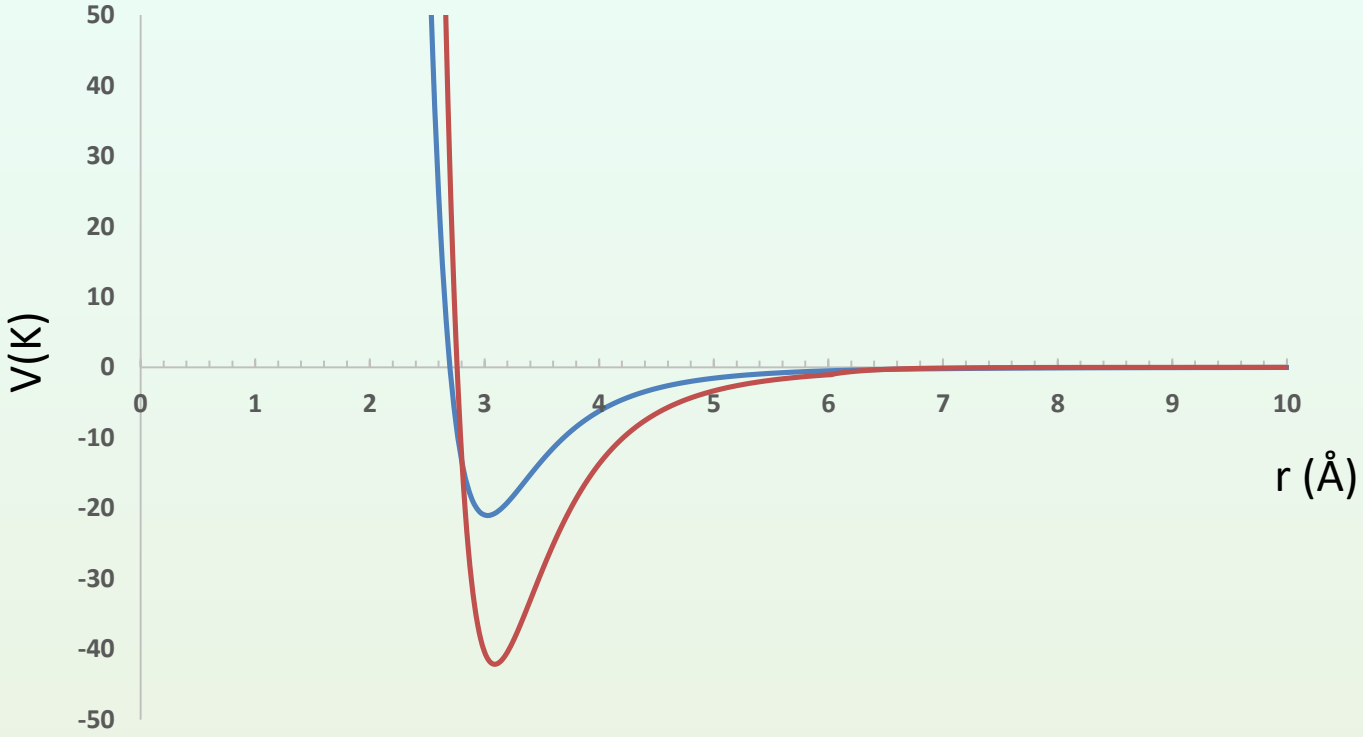

Potential energy curves for the He-He (blue line) and He-Ne (red line) pairs. The pair potential for He-Ne is taken from L.Cacheiro et al. // *Mol. Phys.* 102 *(*2004) 101 and He-He is the HFD-B potential from R.A.Aziz // *Mol. Phys*. 61 (1987) 1487.

Binding Energies $E_{v,J}$ of $^4He^{20}Ne$ and $^4He^{22}Ne$ in Kelvin

$E_{v,J}$	Dimer	experiment	theory
$E_{0,0}$	$^4He^{20}Ne$	–3.71 ± 0.15	-3.713829
	$^4He^{22}Ne$	–4.6 ± 0.8	-3.787811

Experiment - J. Kruse et al. // *J. Phys. Chem. Lett.* 2025, 16, 13, 3225-3231
Theoretical binding energies of this work are computed from the potential of L.Cacheiro et al. // *Mol. Phys.* 2004, *102*, 101−110

The difference between exp. and calc. energies probably related to the statistics of the $^4He^{22}Ne$ data, which is ten times lower than the statistics of $^4He^{20}Ne$.

(4.6 - 0.8) K – (3.71 + 0.15) K = 0.06 K.

Uncertainties and inaccuracies in the fundamental constants can substantially exceed numerical errors. V.Roudnev, M.Cavagnero // J. Phys. B: At. Mol. Opt. Phys. **45** (2012) 025101

INTERACTION POTENTIALS

$^{4}He\ ^{20}Ne$

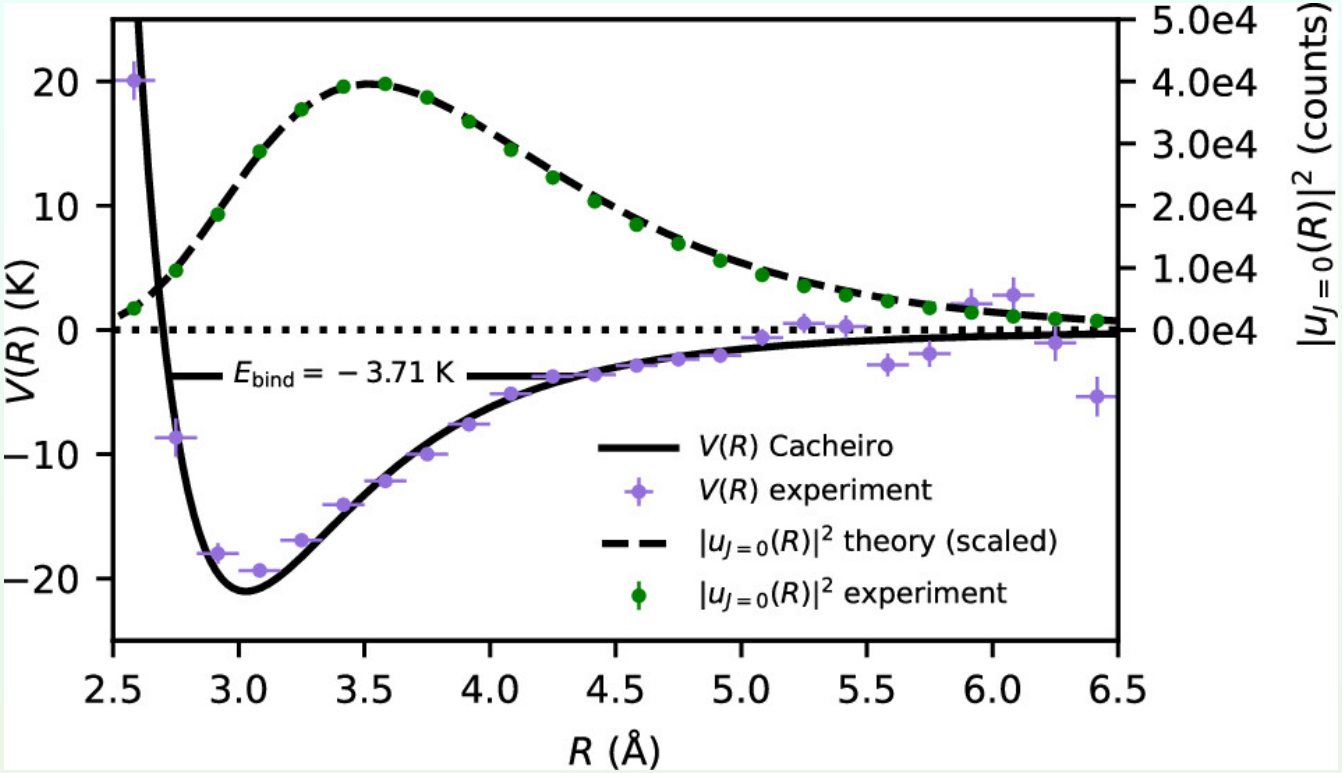

Purple dots represent the helium–neon potential computed from the measured pair distance distribution of $^{4}He^{20}Ne$. Horizontal error bars correspond to the bin width ΔR, the vertical error bar is the statistical error √N of the pair distance distribution (green dots). The black solid line corresponds to the theoretical helium–neon potential of Cacheiro et al. // *Mol. Phys.* 2004, *102*, 101−110

J. Kruse et al. // *J. Phys. Chem. Lett.* 2025, 16, 13, 3225-3231
DOI: (10.1021/acs.jpclett.5c00377)

Calculations

$^{20}Ne_2$

Level	0			1			2		
Potential	E_0	$\langle r \rangle$	$\sqrt{\langle r^2 \rangle}$	E_1	$\langle r \rangle$	$\sqrt{\langle r^2 \rangle}$	E_2	$\langle r \rangle$	$\sqrt{\langle r^2 \rangle}$
TT	24.0598	3.3329	3.3471	4.2049	4.2849	4.3438	0.0181	12.4793	13.8709
HFD-B	24.3715	3.3309	3.3452	4.4527	4.2527	4.3109	0.0276	11.2127	12.2721

Table 1. Energy levels of the bound states E_n (K), the average radius $\langle r \rangle$ (Å) and the root mean square radius $\sqrt{\langle r^2 \rangle}$ (Å) of Ne dimers, calculated with potentials TT [9] and HFD-B [10]. The energies are given in units of K and are relative to the three-body dissociation threshold.

Experiment

n	E (K)[4]
0	24.22 ± 0.02
1	4.405 ± 0.02
2	< 0.14

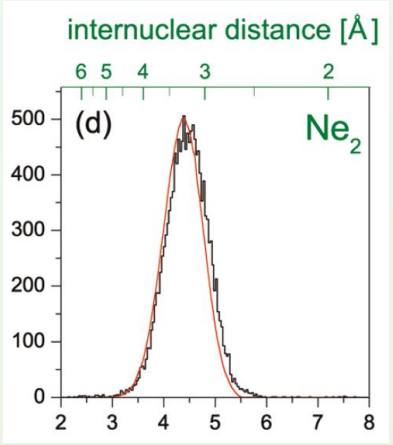

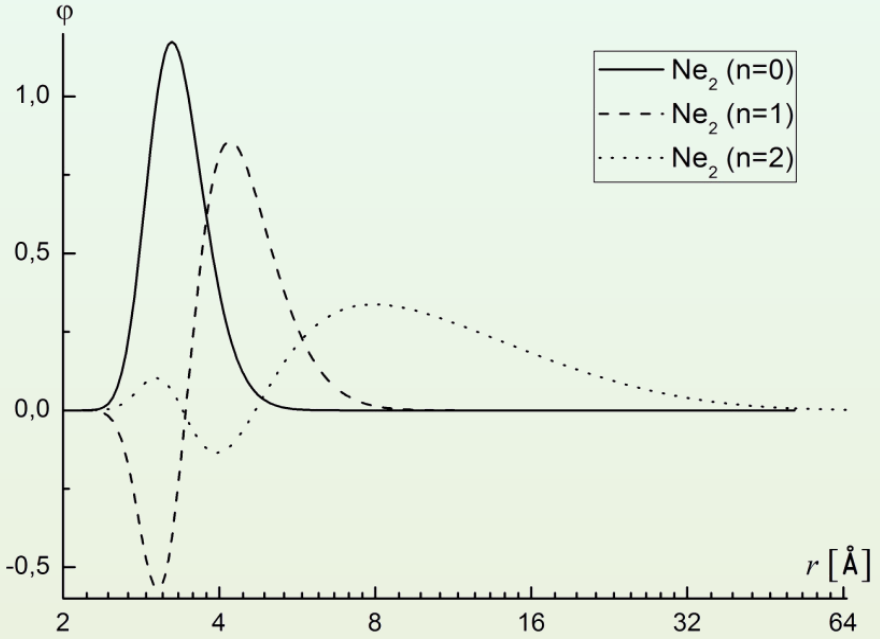

Fig. The radial wave functions φ of the ground and excited states of neon dimer, calculated with the TT potential [9].

[4] A.Wüest, F.Merkt // J.Chem.Phys.118 (2003) 8807.
[5] B. Ulrich et al.//J. Phys. Chem. A 115 (2011) 6936.

[9] K.T. Tang and J.P. Toennies//
J. Chem. Phys. 118, 4976 (2003).
[10] R.A. Aziz and M.J. Slaman//
J. Chem. Phys. 130, 187 (1989).

Helium and Neon dimers

$^4He_2$ Bound state energy - $\varepsilon_d \approx -1.7\ mK$

No rotational J>0 bound states

^3He-^4He does not support bound states

$^4He\ ^{20}Ne$

Bound state energy, J=0 - $\approx -3.7\ K$

Rotational J=1 and 2 bound states $\approx -2.7\ K$ and $-0.76\ K$

$^3He\ ^{20}Ne$

Bound state energy, J=0 - $\approx -2.3\ K$

Rotational J=1 bound states $\approx -1.2\ K$

$^{20}Ne_2$ Three J = 0 bound states - $\approx -24.2\ K, 4.4\ K$ and $0.02\ K$

15 rotational bound states

1 K = 8.6 x 10^{-5} eV

Three – Body Systems

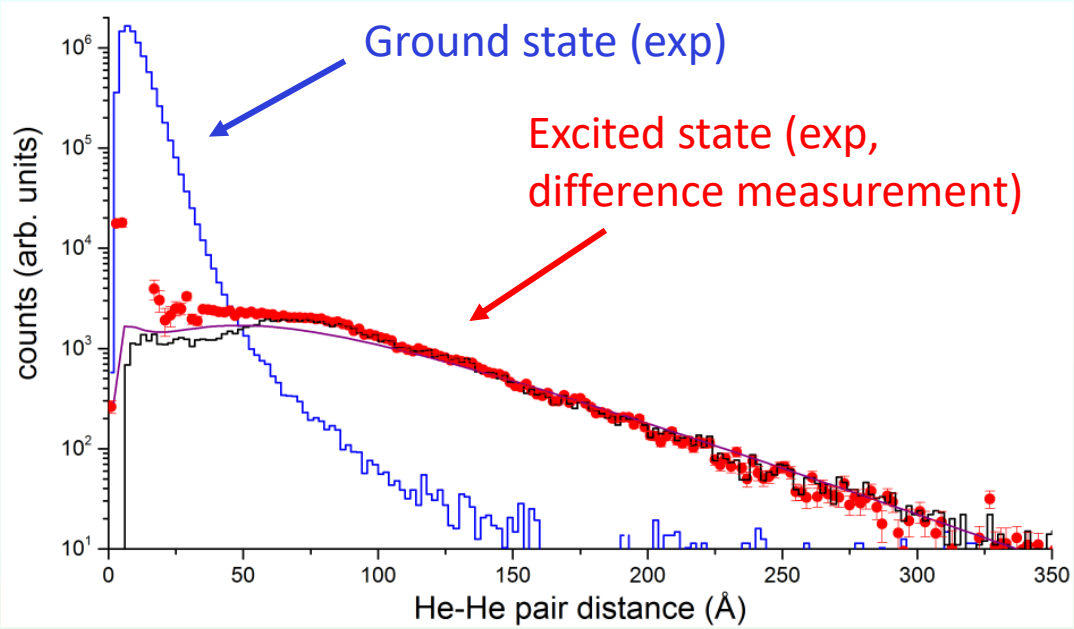

Experimental observation of the Efimov state of the helium trimer. Pair distance distributions $P_{pair}(R)$ of the He_3 excited state. The red circles represent the difference between the mixture of the excited and ground state distribution and the ground state only distribution. The black histogram corresponds to the distribution that was obtained from the measured momenta of the ground and excited state mixture by filtering out the structures with higher KERs. Experimental distributions have been reconstructed from the measured momenta to invert the Coulomb explosion.

$$\varepsilon_d - E^* = 0.98 \pm 0.2\ mK$$

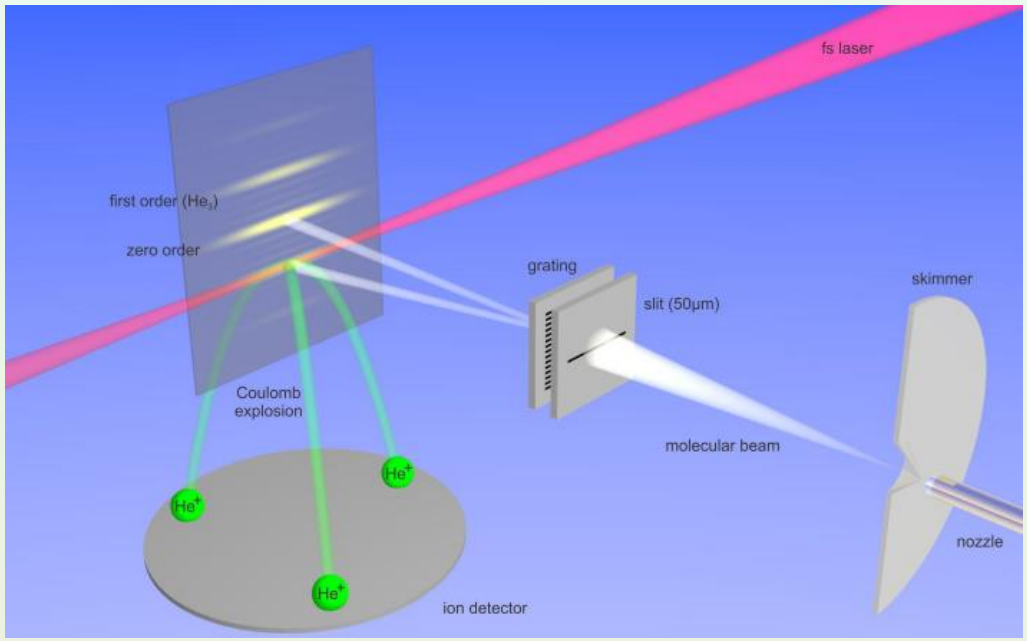

Selection of He trimers from the molecular beam by means of matter wave diffraction.

M.Kunitski et al., *Science* **348**, 551 (2015)

Experiment

$^{20}Ne_3$

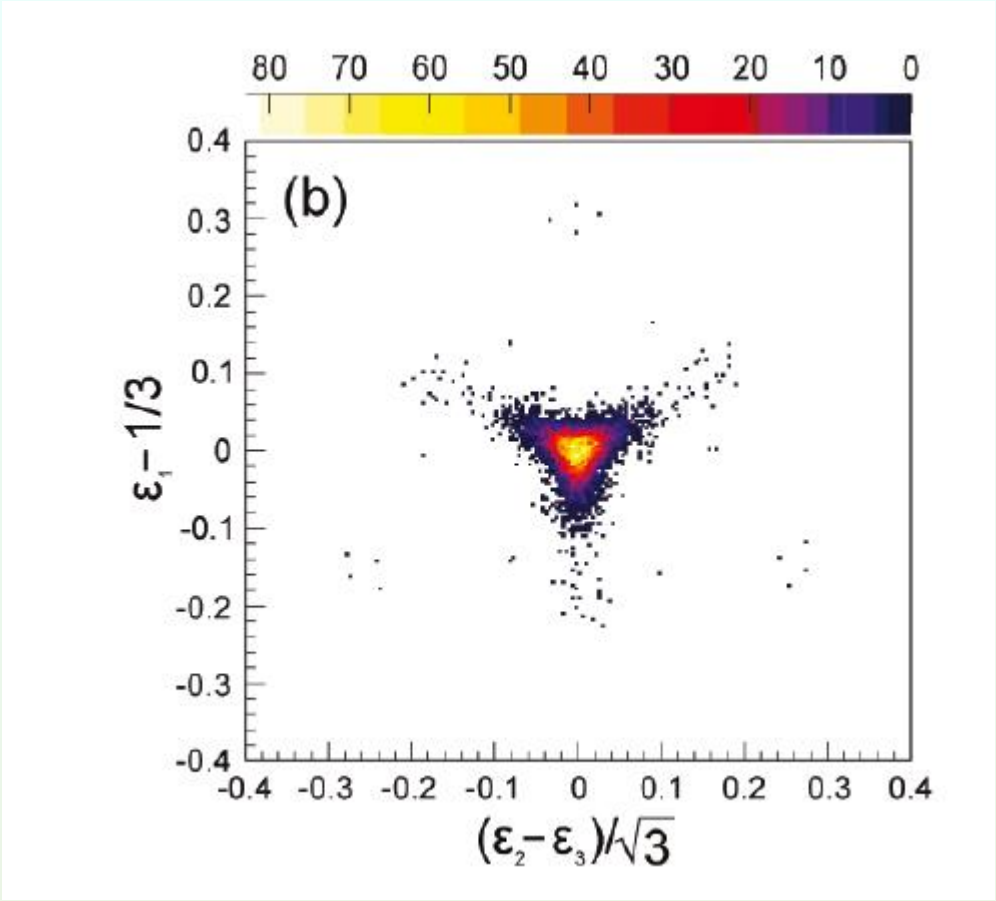

Dalitz plot for the experimental data for the neon trimer

This probability-density plot allows visualizing the full kinematics of a three particle breakup by plotting the relative energy ε of each fragment on an equilateral triangle coordinate system.

B. Ulrich et al.//J. Phys. Chem. A 115 (2011) 6936.

P. Naidon, Sh. Endo, Rep.Prog.Phys. 80 (5) (2017) 056001;

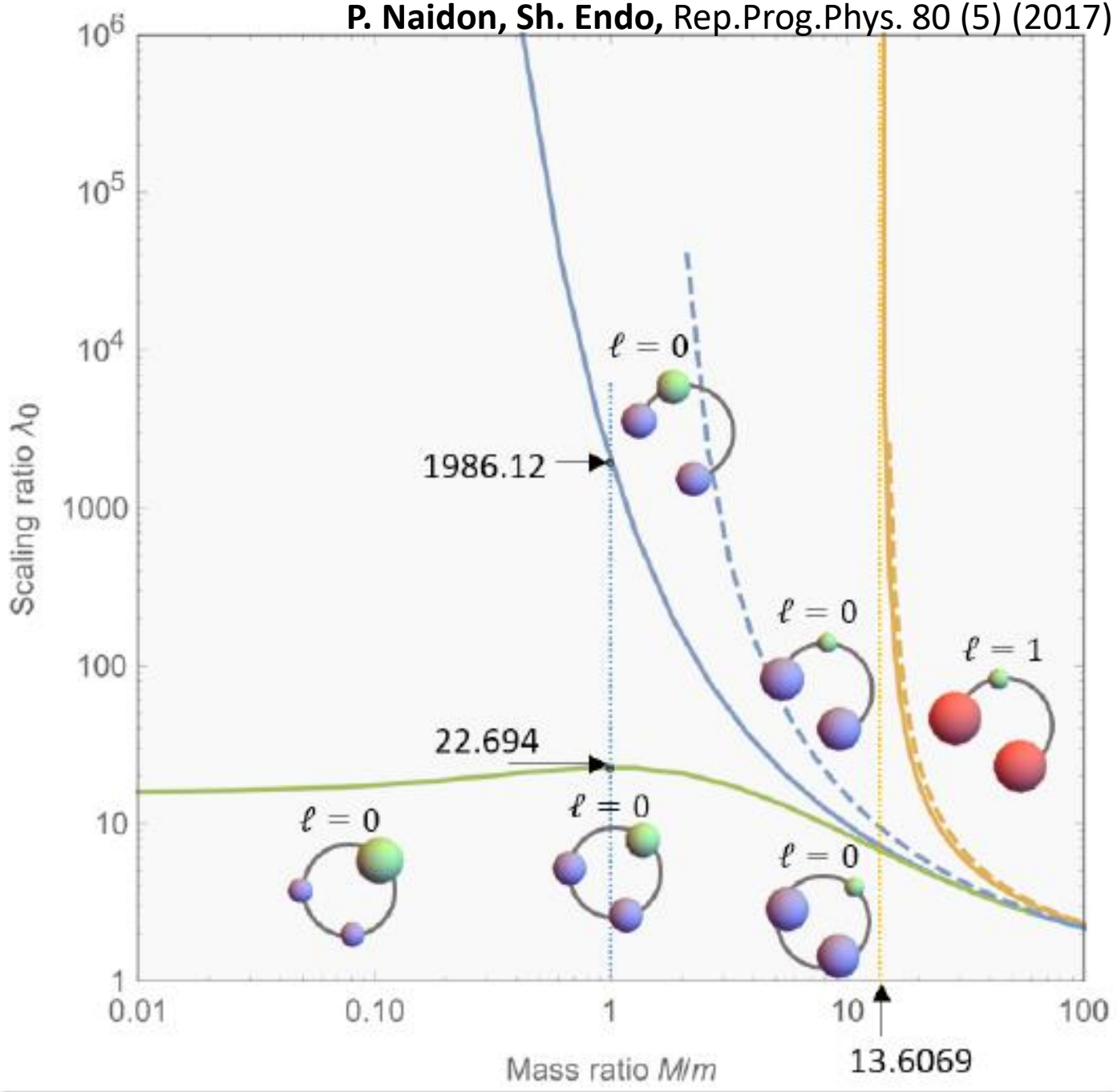

Helium and Neon trimers

$^4He_3$

Two J = 0 bound states - ≈ -131 mK and -2.6 mK

No rotational J>0 bound states

$^3He\ ^4He_2$

One J = 0 bound state ≈ -14.2 mK

$^4He_2\ ^{20}Ne$

Two J = 0 bound states ≈ -7.3 K and -4.4 K

$^3He_2\ ^{20}Ne$

One J = 0 bound state ≈ -4.8 K

$^3He\ ^4He\ ^{20}Ne$

One J = 0 bound state ≈ -6.0 K

Shahzad, Li // Phys. Rev A **90**, 032510 (2014)

$^{20}Ne_3$

E (K)	HFD-B	TT	[1]^a	[2]^a
E_0	74,13	74,07	74,10	74,11
E_1	52,44	52,37	52,41	52,43
E_2	49,25	49,19	49,23	49,24
E_3	45,53	45,49	45,51	45,52
E_4	40,37	40,31	40,34	40,35
E_5	34,67	34,62	34,65	34,66
E_6	32,33	32,27	32,3	32,31
E_7	31,54	31,48	31,51	31,52
E_8	27,66	27,61	27,64	27,65
E_9	26,20	26,16	26,17	26,18
E_{10}	24,95	24,92	24,93	25,02

a – HFD-B potential model used.

[1] M. Salci, S. B. Levin, N. Elander, and E. Yarevsky, J. Chem. Phys. **129**, 134304 (2008).
[2] H. Suno, J. Chem. Phys. **135**, 134312 (2011); *ibid*, J. Phys. B **49**, 014003 (2016).

Summary

- Helium and Neon small clusters can be experimentally realized, and their structures can even be studied. The experimental observation would be more than welcome, also for other atoms! Connections to experiments have been and will continue to be very important.

- Few-body physics can help answer fundamental questions in an unambiguous, clean, and precise way. Accurate calculations are needed.

Thank you for your attention